

This article was downloaded by: [Tomsk State University of Control Systems and Radio]

On: 19 February 2013, At: 14:32

Publisher: Taylor & Francis

Informa Ltd Registered in England and Wales Registered Number: 1072954

Registered office: Mortimer House, 37-41 Mortimer Street, London W1T 3JH, UK



Molecular Crystals and Liquid Crystals

Publication details, including instructions for authors and subscription information:

<http://www.tandfonline.com/loi/gmcl16>

Model Compounds of Main-Chain Thermotropic Nematic Polyesters

R. B. Blumstein^a, M. D. Poliks^a, E. M. Stickles^a,
A. Blumstein^a & F. Volino^b

^a Polymer Science Program, Department of Chemistry, University of Lowell, Lowell, MA, 01854

^b CNRS and DRF, Service de Physique, CENG 85X, 38041, Grenoble, Cedex, (FRANCE)

Version of record first published: 19 Oct 2010.

To cite this article: R. B. Blumstein, M. D. Poliks, E. M. Stickles, A. Blumstein & F. Volino (1985): Model Compounds of Main-Chain Thermotropic Nematic Polyesters, *Molecular Crystals and Liquid Crystals*, 129:4, 375-407

To link to this article: <http://dx.doi.org/10.1080/00268948508085039>

PLEASE SCROLL DOWN FOR ARTICLE

Full terms and conditions of use: <http://www.tandfonline.com/page/terms-and-conditions>

This article may be used for research, teaching, and private study purposes. Any substantial or systematic reproduction, redistribution, reselling, loan, sub-licensing, systematic supply, or distribution in any form to anyone is expressly forbidden.

The publisher does not give any warranty express or implied or make any representation that the contents will be complete or accurate or up to date. The accuracy of any instructions, formulae, and drug doses should be

independently verified with primary sources. The publisher shall not be liable for any loss, actions, claims, proceedings, demand, or costs or damages whatsoever or howsoever caused arising directly or indirectly in connection with or arising out of the use of this material.

MODEL COMPOUNDS OF MAIN-CHAIN THERMOTROPIC NEMATIC POLYESTERS

R. B. BLUMSTEIN, M. D. POLIKS, E. M. STICKLES and A. BLUMSTEIN

Polymer Science Program, Department of Chemistry, University of Lowell, Lowell, MA 01854

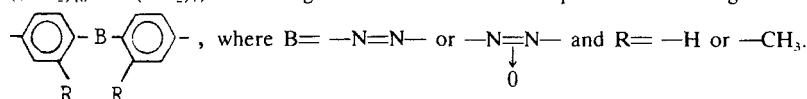
and

F. VOLINO

CNRS and DRF, Service de Physique, CENG 85X, 38041 Grenoble Cedex (FRANCE)

(Received October 12, 1984)

Investigation of precursors of thermotropic nematic polyesters with flexible spacers $((\text{CH}_2)_{10}$ and $(\text{CH}_2)_7$) and mesogens in the main chain is reported. The mesogens are

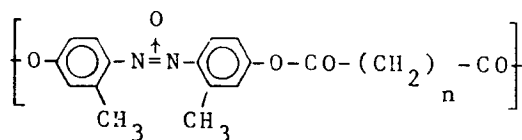


Mixtures of structural isomers of 2,2'-dimethylazoxybenzene derivatives display broad multiple melting. Several types of sequencing of mesogen and spacer were investigated. Compounds formed by the sequence mesogen-central spacer-mesogen appear to provide an adequate model of polymeric behavior. Influence of mesogen and spacer on phase transition entropies and mesogen nematic order parameter, as well as temperature dependence of alkyl chain flexibility were investigated in selected compounds. These can also serve as models for study of mesophase glasses and the semicrystalline state of nematic polymers.

INTRODUCTION

We have reported previously on the investigation of thermotropic nematic polyesters formed by alternating flexible spacer groups and rigid mesogenic moieties based on azoxybenzene.¹ Attention was

focused on the homologous series represented by

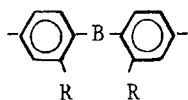


and formed by condensation of 2,2'-dimethyl-4,4'-dihydroxyazoxybenzene (subsequently called mesogen "9") with diacid chlorides containing a methylene sequence length $n = 2-14$. This series is characterized by a strong and regularly sustained odd-even effect, with polymers in which $n = \text{even}$ displaying a higher degree of order than is usually found in low molecular mass (LMM) nematics.² On the strength of X-ray diffraction patterns of quenched aligned mesophases, a micellar cybotactic nematic model was proposed for the $n = \text{even}$ members of the series.^{3,4} In the case of the odd-numbered spacers, the polymers display an ordinary nematic organization.

While the even-odd nature of the spacer provides the driving force for mesophase organization, it is the orientational contribution of the mesogen that is largely responsible for the high level of nematic order in the $n = \text{even}$ series. This can be inferred from consideration of the entropies of isotropization,⁴ and from the regular oscillation of the nematic order parameters S associated with the mesogens.⁵ Although spacer flexibility appears to increase significantly as the nematic-isotropic (N/I) transition is approached,⁶ mesogen order appears to be stabilized throughout the entire nematic phase, relative to LMM nematics.⁵

In a preliminary investigation,⁷ we have reported the synthesis of model compounds and oligomers of a polymer based on mesogen "9" and the diacid chloride of 1,12-dodecanedioic acid ($n = 10$). This polymer is subsequently designated as DDA9. The model compound of the repeating unit, formed by a rigid-flexible (RF) sequence, is not mesomorphic. Oligomers with flexible tails are not mesomorphic below a chain length of some five repeating units. However, a model compound consisting of a spacer moiety enclosed between two terminal mesogen units (RFR sequencing) forms a monotropic nematic phase. In other words, the enantiotropic mesophase in polymer DDA9 forms as a result of cooperativity between about five repeating units. The polymer is characterized by a strong "plateau effect," namely it displays a rapid build-up of order with leveling off at about 10 repeating units per chain.^{8,9}

In the present paper, we report a detailed investigation of model compounds based on four different mesogens of general formula



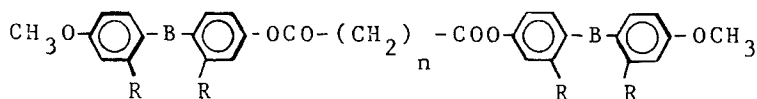
where R = H and B = $\text{---} \text{N} \begin{array}{c} \text{O} \\ \uparrow \end{array} \text{N} \text{---}$ (mesogen 8)

R = CH₃— and B = $\text{---} \text{N} \begin{array}{c} \text{O} \\ \downarrow \end{array} \text{N} \text{---}$ (mesogen “9”)

R = H— and B = $\text{---} \text{N} \text{=N} \text{---}$ (mesogen 8’)

R = CH₃— and B = $\text{---} \text{N} \text{=N} \text{---}$ (mesogen 9’).

Particular consideration will be given to compounds with RF sequencing (models of repeating unit) and to “siamese twin”¹⁰ compounds with RFR sequencing of general formula



where $n = 10$ (spacer DDA) and $n = 7$ (spacer AZA, derived from azelaic acid). These compounds are similar in sequencing to the azobenzene derivatives with $n = 0\text{--}8$ first reported by Vorländer.¹¹ They can be considered as the first oligomers in the ascending series of molecular weights inasmuch as their flexible moiety is doubly linked to mesogens, which allows for intramolecular correlations between mesogens, as is the case in the corresponding polymers. The qualitative resemblance between behavior of RFR-type models and their polymeric counterparts will be discussed.

EXPERIMENTAL SECTION

Synthesis of Intermediate Compounds

The 4,4’-hydroxyazoxybenzene (mesogen 8) and 2,2’-dimethyl-4,4’-hydroxyazoxybenzene (mesogen “9”) were prepared according to literature procedures,^{12,13} modified to improve yield.¹⁴ Intermediates

I (2,2'-dimethyl-4-hydroxy-4'-methoxyazobenzene) and II (a mixture of structural isomers 4-methoxy-4'-hydroxy-2,2'-dimethyl-ONN-azoxybenzene [(IIa)] and 4-methoxy-4'-hydroxy-2,2'-dimethyl-NNO-azoxybenzene [(IIb)]) were prepared as in reference 7.

Intermediates III (4-hydroxy-4'-methoxyazobenzene) and IV (a mixture of 4-hydroxy-4'-methoxy-ONN-azoxybenzene and 4-hydroxy-4'-methoxy-NNO-azoxybenzene) were prepared in a similar fashion. Intermediate V (a mixture of structural isomers of 4-hydroxy-4'-lauroyloxy-2,2'-dimethylazoxybenzene) was prepared as in reference 7.

Separation of structural isomers IIa and IIb was carried out by a) column chromatography using Woelm silica with chloroform (0.75% ethanol) as mobile phase; b) by repeated fractional recrystallization from isopropanol.

Synthesis of Model Compounds with RF Sequencing

Model 9DDA (2,2'-dimethyl-4-methoxy-4'-lauroyloxyazoxybenzene in a mixture of ONN and NNO structural isomers) was prepared from intermediate II as described in reference 7. Model 9AZA (2,2'-dimethyl-4-methoxy-4'-nonoyloxyazoxybenzene in a mixture of ONN and NNO structural isomers) was prepared in similar fashion.

Synthesis of Model Compounds with RFR Sequencing

Model compound 9DDA9-M (a mixture of three structural isomers: bis-4-(4'-methoxy-2,2'-dimethyl-NON-azoxybenzene)-1,12-dodecanedioate was prepared as in reference 7. Model compound ONN-9DDA9 (structural isomer bis-4-(4'-methoxy-2,2'-dimethyl-ONN-azoxybenzene)-1,12-dodecanedioate) was prepared according to the same procedure from intermediate IIa. Compound ONN-9DDA9-d₂₀ (bis-4-(4'-methoxy-2,2'-dimethyl-ONN-azoxybenzene)-1,12-d₂₀-deuterododecanedioate) was prepared from intermediate IIa and the diacid chloride of 1,12-d₂₀-deuterododecanedioic acid (from Merck, Sharp and Dome Isotopes of Canada).

Compounds 8DDA8-M (bis-4-(4'-methoxy-NON-azoxybenzene)-1,12-dodecanedioate), 8'DDA8' (bis-4-(4'-methoxyazobenzene)-1,12-dodecanedioate), and 9'DDA9' (bis-4-(4'-methoxy-2,2'-dimethylazobenzene)-1,12-dodecanedioate) were similarly prepared from the diacid chloride of 1,12-dodecanedioic acid and intermediates IV, III and I, respectively.

Compound NNO-9AZA9 (bis-4-(4'-methoxy-2,2'-dimethyl-azoxybenzene)-1,9-azelaioate) was prepared from intermediate IIb and the diacid chloride of azelaic acid.

Synthesis of Symmetrically Substituted Model Compounds

Compounds Ac8Ac (4,4'-acetoxyazoxybenzene), Ac9Ac (2,2'-dimethyl-4,4'-acetoxyazoxybenzene) and DDA9DDA (2,2'-dimethyl-4,4'-lauroyloxyazoxybenzene) were prepared from mesogens "8" and "9" as described in reference 7. Diol 10 (4,4'-bis-(2-hydroxyethyl)azoxybenzene) was prepared by an oxidation of p-aminophenethyl alcohol using hydrogen peroxide and acetonitrile, by a procedure analogous to that reported for dialkyl azoxybenzenes.¹⁵

Synthesis of Siamese Twin Oligomer

Compound (DDA9)₂-DDA(4-(4'-lauroyl-2,2'-dimethyl-NON-azoxybenzene)-1,12-dodecanedioate) was prepared from intermediate V as in reference 7.

Characterization

Sample purity was checked by means of the standard techniques such as elemental analysis, thin layer chromatography (TLC), high performance liquid chromatography. A typical example is given for sample 9DDA9-M:

TLC

SiO₂ Plate (adsorption): 1 spot

Reversed Phase Plate (solubility): 1 spot

Elemental Analysis

Element	Calculated (%)	Found (%)
C	68.27	68.12
H	6.82	6.90
N	7.58	7.44

Samples were further characterized by polarizing microscopy, differential scanning calorimetry (DSC) and high resolution PMR spectroscopy as described in references 8 and 9, which treated characterization of oligomers. Sample thermal history was carefully controlled. Unless specified, all scanning rates were 10°/min., with samples cycled between ~ 20° beyond isotropization temperature and 240° K.

In the thermal optical analysis experiments (TOA) intensity of transmitted light was measured using a photodiode attachment to the microscope. Broad line PMR experiments were performed on a CXP-100 Brüker spectrometer working at 75 MHz and deuterium NMR on a WM-250 Brüker spectrometer working at 38.4 MHz. The samples were degassed and sealed under vacuum in 5 mm tubes. Following equilibration for 40 min. at a temperature ~ 20° above isotropization, the samples were cooled slowly in steps of 2–3°. The nematic

order parameter S associated with the mesogen was deduced from the main dipolar splitting $2\delta N$ of samples containing mesogen "9," as described in reference 16 (see inset of Figure 13). The nematic fraction f_n in the nematic-isotropic biphasic and the fraction of total intensity contained in the broad component of the solid phase spectra were deduced either from the FID signals or from the spectra as described in reference 17, where additional information can be found concerning experimental procedure.

RESULTS

Structure-Property Relations: Comparison with Corresponding Polymers

In Table I are listed phase transition temperatures of model compounds synthesized in this work along with some representative systems taken from the literature. Compounds in Table I are classified as follows:

- Compounds a–d are symmetrically substituted molecules with a mesogenic core.
- Compounds e–h are 4-methoxy-4'-acyloxy substituted mesogens, with a rigid-flexible (RF) sequencing.
- Compound i is a siamese twin structure with a flexible core and a FRFRF sequence of flexible and rigid units.
- Compounds j–p are siamese twin structures with a flexible core and a rigid-flexible-rigid (RFR) sequence of structural units.
- The suffix M refers to mixtures of structural isomers in unsymmetrically substituted derivatives of azoxybenzene.

Phase transitions of models are dominated by the structure of the mesogen, as is usual in standard LMM compounds. Thus, lateral substitution in the mesogen destroys or disturbs the mesophase as is obvious from comparison of:

- a) Compounds j and k: 9'DDA9' (K118I) and 8' DDA8' (K148S162N 208I)
- b) Compounds m and l: 9DDA9 (monotropic nematic) and 8DDA8 (K146N214I)
- c) Compounds b and c: Ac8Ac (narrow monotropic nematic phase) and Ac9Ac (K151I).

It should be noted that Ac8Ac (4,4'-acetoxiazoxybenzene) is reported in reference 18 as displaying a narrow enantiotropic nematic phase. This discrepancy between our data and literature data is probably due to a difference in purity between the two samples, as pres-

TABLE I
Phase Transitions of Model Compounds (in °C).

			Reference (14)
a.	Diol 10		K96.5N103.5I
b.	Ac8Ac		K169I (152.5N150K) K163N166I
c.	Ac9Ac		K151I
d.	DDA9DDA		K77I
e.	_____		K72N114I (19)
f.	_____		K76N99I (19)
g.	9DDA-M		K41.4, 59.4I

TABLE I continued

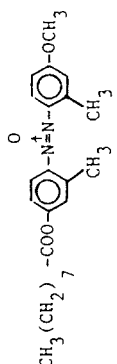
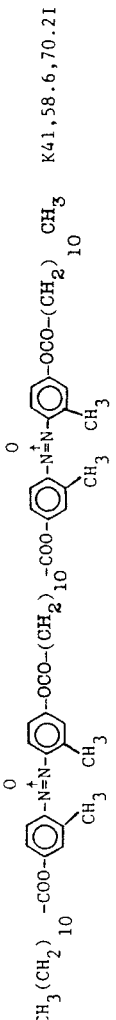
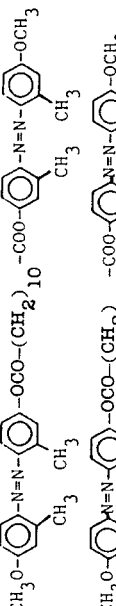
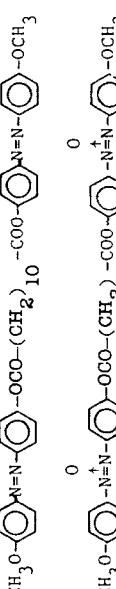
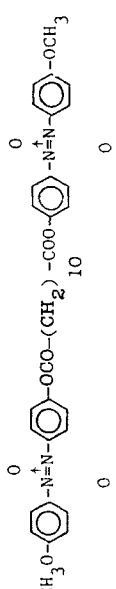
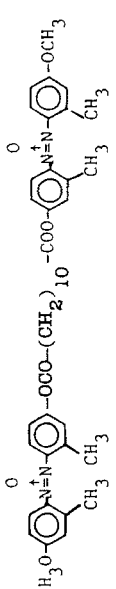
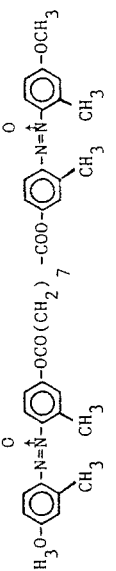
h.	9AZA-M		K32.3, 39.9I
i.	(DDA9) ₂ DDA-M		K41, 58.6, 70.2I
j.	9'DDA9'		K118I
k.	8'DDA8		K148S162N208I
l.	8DDA8-M		K146N214I
m.	9DDA9-M		K92*, 112, 122I (1100N632K)
n.	NNO-9AZA9		K103I(178N-5 g)

TABLE I continued

o.	ONN-9DDA9		K112I (199N85K)
p.	ONN-9DDA9-d ₂₀		K110I (197N81K)

* The endotherm at 92° C may correspond to the K/N transition of hybrid isomer ONN/NNO, but this could not be ascertained.

ence of small amounts of impurity tends to transform a monotropic phase into an enantiotropic one.

RFR-type models based on mesogen "9" are monotropic nematics (compounds m-p). Comparison of ONN-9DDA9 and ONN-9DDA9-d₂₀ shows a lowering of phase transition temperatures consistent with the isotropic labeling of the spacer group in ONN-9DDA9-d₂₀.

Structure property behavior in the corresponding polymers is somewhat more complex, as illustrated in Table II. Lateral substitution in the azoxybenzene moiety lowers the phase transition temperatures without decreasing the width of the mesophase. This can be seen by comparing behavior of polymers based on mesogen "8" and "9". In contrast, lateral disubstitution in the azobenzene moiety (mesogen 9') completely destroys the mesophase, as it does in the corresponding RFR model compound.

TABLE II
Phase Transition Temperatures of Related Polymers (in °C).

$\left[\text{R}-\text{OCO}(\text{CH}_2)_n\text{COO} \right]$			
<u>R</u>	<u>n</u>		<u>Reference</u>
Mesogen 8	7	² K22N271I	(21)
	10	K216N265I	(3)
Mesogen 9	7	K92N156I	(2)
	10	K118.2N163.5I	(3)
Mesogen 10	7	K140I	(21)
Mesogen 8'	7	K211N250I	(21)
Mesogen 9'	7	K140I	(21)

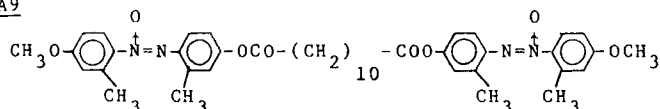
Finally, the polymer based on nematic mesogen "10" is not mesomorphic, in agreement with our previous observation²⁰ that removal of ester group to the interior of the spacer destroys liquid crystalline behavior in the polymer.

Identification of Structural Isomers

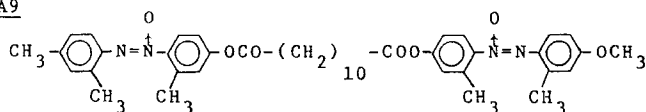
Structural assignments were made on the basis of high resolution PMR spectra. Representative chemical shift assignments are summarized in Table III. The aromatic and aliphatic portions of the 250 MHz PMR spectrum of 9DDA9 and ONN-9DDA9 are shown in Figures 1 and 2. It is apparent that structural isomerism is reflected in both regions of the spectrum, i.e., the proportions of ONN and NNO sequences in 9DDA9 can be computed from the relative intensities at locations 3' and 4 in the aromatic portion of the spectrum and/or at locations 2 and 3 in the aliphatic chemical shift region, for example.

Compound 9DDA9-M is a mixture of three structural isomers;

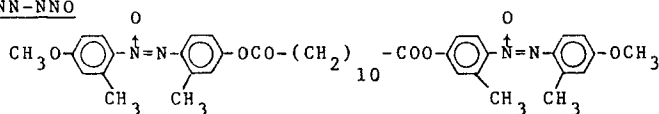
ONN-9DDA9



NNO-9DDA9



Hybrid ONN-NNO

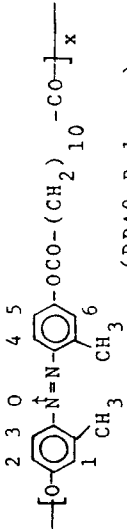
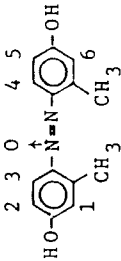
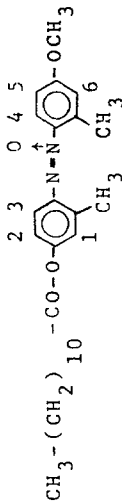
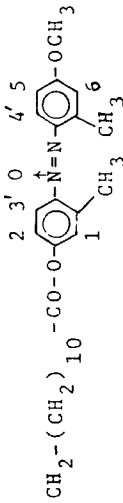


The relative amounts of the three structural isomers can be computed from the NMR spectrum by assuming a statistical distribution of ONN and NNO sequences.

Multiple Melting in Unsymmetrically Substituted Derivatives of Mesogen "9"

Table I shows that 9DDA, 9AZA, (DDA9)₂-DDA, and 9DDA9-M, which are unsymmetrically substituted derivatives of mesogen "9," show multiple melting peaks at the K/I transition. This is illustrated

TABLE III
Proton NMR Peak Assignments.

	δ_1	δ_2	δ_3	δ_4	δ_5	δ_6
	7.02	7.02	8.38	7.68	7.02	7.02
	6.77	6.77	8.47	7.57	6.77	6.77
	7.00	7.00	7.63	8.26	6.80	6.80
	δ_1	δ_2	δ_3	δ_4	δ_5	δ_6
	7.00	7.00	8.68	7.63	6.80	6.80



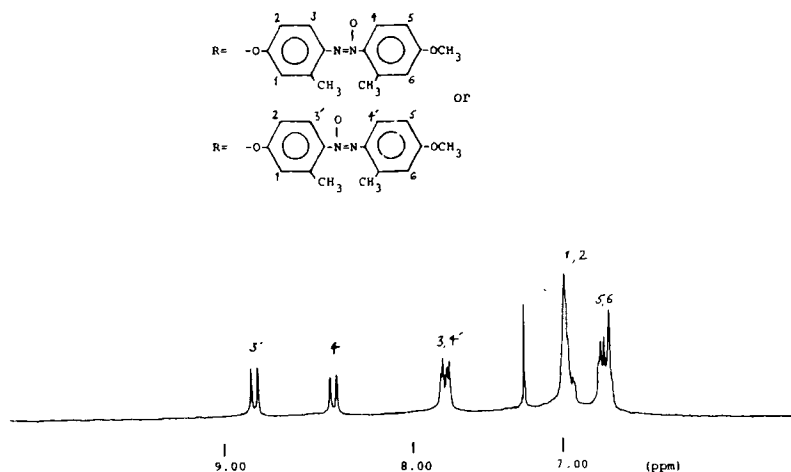


FIGURE 1 Aromatic portion of the 250 MHz PMR spectrum of 9DDA9-M (Solvent: chloroform, at 7.26 ppm).

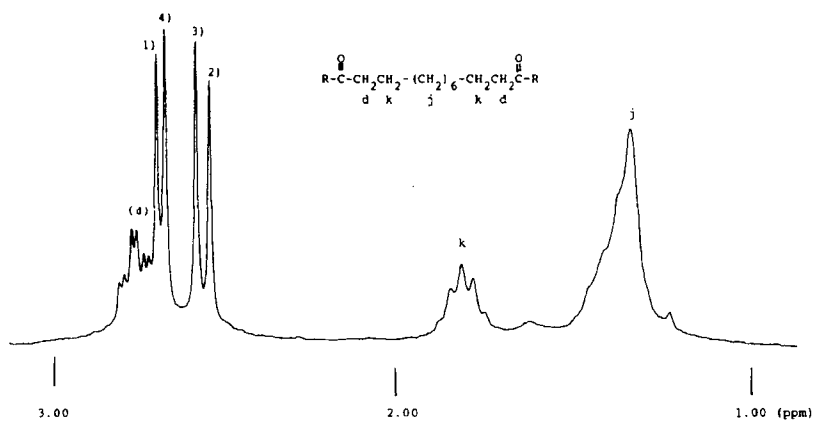
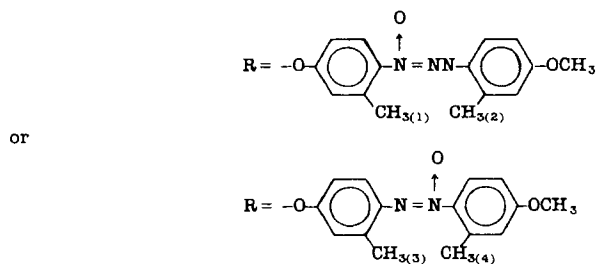


FIGURE 2 Aliphatic portion of the 250 MHz PMR spectrum of 9DDA9-M



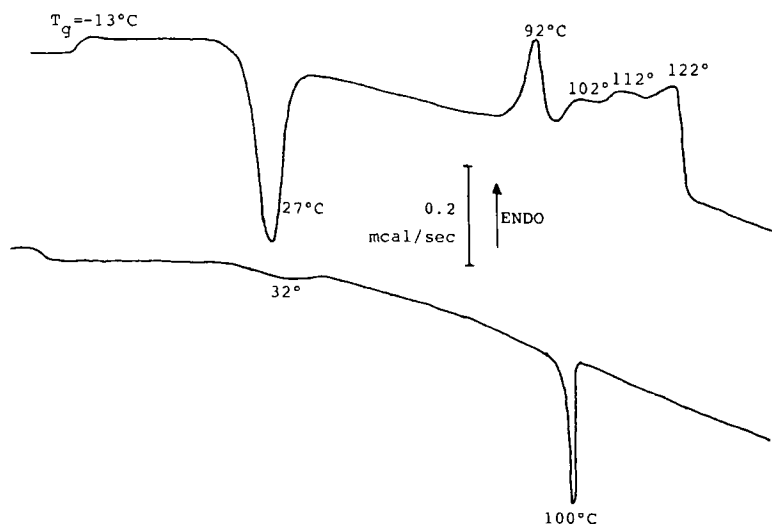


FIGURE 3 DSC thermogram of 9DDA9-M. Upper curve: heating; Lower curve: cooling.

in Figure 3, which shows the DSC thermogram for 9DDA9-M upon heating and cooling. Pure structural isomers of 9DDA9, on the other hand, display sharp melting behavior at the K/I transition. Figure 4, for example, shows the DSC thermogram of ONN-9DDA9 with a sharp K/I transition on heating and N/K on cooling. This is in contrast to the extremely sluggish crystallization of 9DDA9-M on cooling. Upon reheating, the supercooled nematic phase of 9DDA9-M undergoes a glass transition (T_g) at -13°C , followed by cold crystallization (peak maximum at 27°C) and four endotherms, at 92° , 102° , 112° and 123°C . The endotherm at 102°C is attributed to the N/I transition of the residual nematic phase trapped within the semicrystalline material. This peak disappears following 12 hours of annealing at 57°C , and it is the only one remaining under thermal cycling conditions where crystallization is prevented. The remaining endotherms correspond to melting transitions of the hybrid ONN-NNO, and isomers ONN and NNO, in that order. Similar multiple melting behavior is observed for the other unsymmetrically substituted derivatives of mesogen "9" listed in Table I.

On the other hand, compound 8DDA8-M, which is an unsymmetrically substituted derivative of azoxybenzene, displayed no multiple melting although NMR indicates the presence of a mixture of structural isomers. This is in agreement with literature data concerning other unsymmetrically substituted derivatives of azoxybenzene,

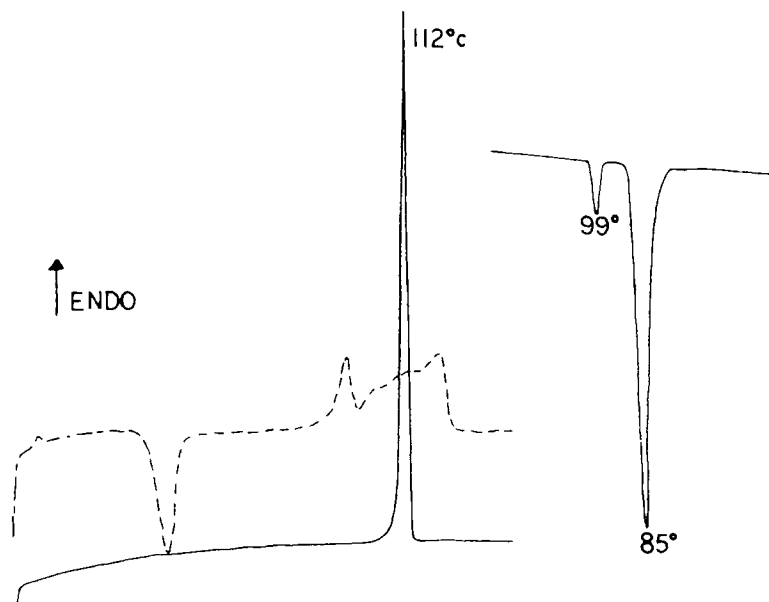


FIGURE 4 Comparison between melting of 9DDA9-M and ONN-9DDA9. *Dashed Line:* heating curve for 9DDA9-M. *Solid line:* heating (left) and cooling (right) curves for ONN-9DDA9

such as compound 5 in Table I. The wide melting span observed in the case of mesogen "9" appears to be due to the lateral substitution at the 2 and 2' positions. Presumably, the crystalline lattice in the 2,2'-dimethyl substituted derivatives has different symmetry in different isomers. In the case of poly(2,2'-dimethyl-4,4'-dioxy-NON-azoxybenzene dodecanedioyl) - polymer DDA9-, where the mesogen is symmetrically substituted at the 4 and 4' positions, except at chain ends, simulation of the PMR spectrum of the macroscopically aligned mesophase suggests that the preferred mesogen conformation has both methyl groups on the same side of the molecule with a dihedral angle between benzene rings of $\sim 36^\circ$.¹⁶ Structural isomerism may modify this dihedral angle and, consequently, the geometry of packing, though in the absence of crystallographic data on single crystals, one can but speculate on this point.

Certainly, Table IV shows that the wide angle X-ray spacings are not the same in 9DDA9-M and in ONN-9DDA9. It further indicates, in agreement with the cold crystallization exotherm shown in Figure 3, that crystallization in 9DDA9-M is improved on heating from the supercooled semicrystalline phase. Similar cold crystallization is observed in mixtures of structural isomers 9DDA-M and 9AZA-M.

TABLE IV

X-ray Spacings of 9DDA9-M as a Function of Temperature (a,b,c) and of ONN-9DDA9-d₂₀ at 30°C (d).

(a) T = 30°C	(b) T = 92°C	(c) T = 102°C	(d) T = 30°C
---	11.4 (w)	11.4 (w)	11.1 (s)
10.12 (s)	10.3 (s)	10.3 (s)	
7.28 (s)	7.32 (w)	7.32 (w)	7.45 (s)
6.55 (w)	6.55 (s)	6.52 (s)	6.71 (s)
---	5.56 (w)	5.58 (w)	5.42 (s)
5.09 (s)	5.17 (s)	5.17 (s)	5.19 (w)
4.83 (w)	4.83 (w)	4.84 (w)	---
---	4.64 (w)	4.64 (w)	4.65 (w)
---	4.25 (w)	4.25 (w)	4.38 (s)
3.82 (s)	3.83 (s)	3.83 (s)	3.91 (w)
---	3.71 (s)	3.71 (w)	3.69 (w)
3.52 (w)	3.52 (w)	3.52 (w)	---
3.26 (w)	3.26 (w)	3.26 (w)	3.29 (w)
---	3.04 (w)	3.04 (w)	---

s: sharp

w: weak

Cold crystallization 9DDA9-M results in a spherulitic morphology, as illustrated in Figure 5, whereas a structural isomer such as ONN-9DDA9 crystallizes sharply on cooling from the nematic melt into needle-like crystals (Figure 6). The spherulitic morphology in 9DDA9-M remains intact until melting of the highest melting isomer, and only the intensity of transmitted light (monitored by thermal optical analysis) changes continuously throughout the K/I transition (Figure 7).

The Nematic-Isotropic Transition

In Table V are listed the enthalpies and entropies of isotropization of selected model compounds and corresponding polymers. It is clear that entropy change at the N/I transition is dominated by the odd-



FIGURE 5 Ringed spherulites formed during cold crystallization of 9DDA9-M; magnification $\times 320$.

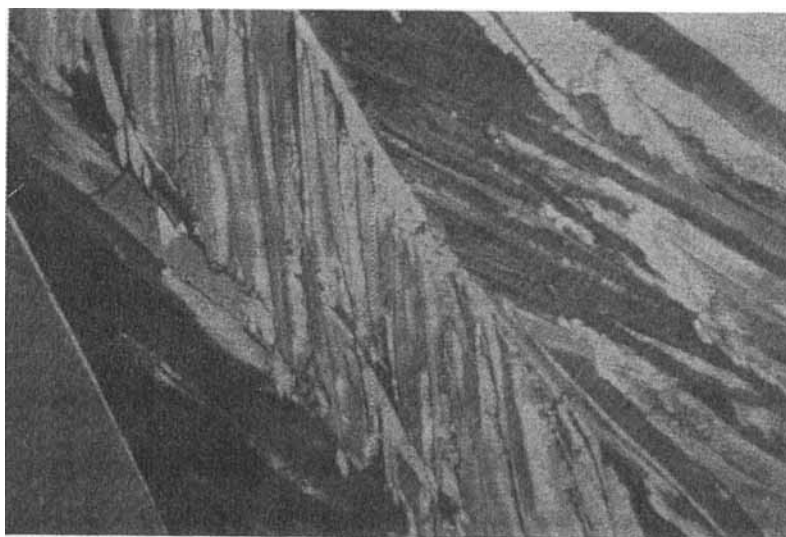


FIGURE 6 Needle-like crystals formed by crystallization of ONN-9DDA9 from the melt; magnification $\times 320$

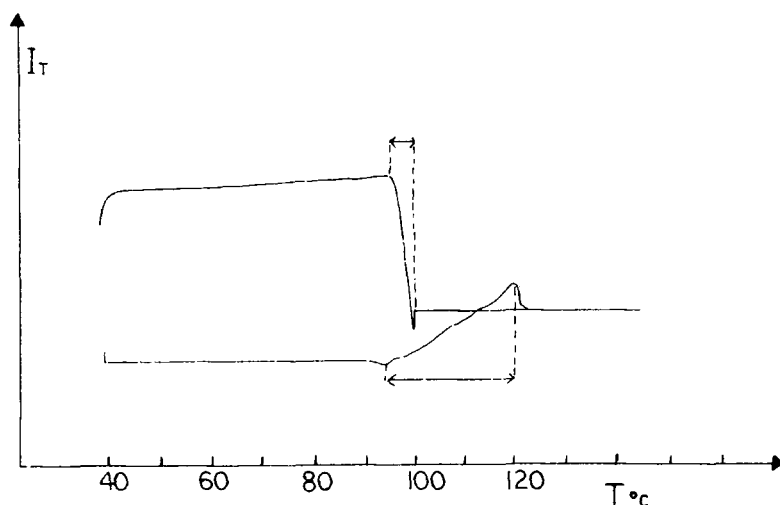


FIGURE 7 Transmitted light intensity (in arbitrary units) as a function of temperature for 9DDA9-M. Upper curve: cooling; lower curve: heating. The biphasic regions are enclosed between arrows.

even nature of the spacer in RFR model compounds and in the polymers, but not in RF compounds.

In RFR models based on spacer DDA ($n = 10$), the values of $\Delta H_{N/I}$ and $\Delta S_{N/I}$ are rather high in comparison with a standard LMM nematic such as p-azoxyanisole (PAA), as reported previously for 9DDA9-M;⁸ in the case of 9AZA9 ($n = 7$), on the other hand, $\Delta H_{N/I}$ and $\Delta S_{N/I}$ are somewhat lower than in PAA.

The last two compounds listed in Table V are azoxybenzene (mesogen "8") derivatives with RF sequencing and odd-even spacer length alternation. We can see that such structures do not adequately model polymeric behavior.

A characteristic feature of the N/I transition in RFR models based on spacer DDA ($n = 10$) seems to be the presence of a nematic-isotropic ($N + I$) biphase. This biphase can be followed by thermal optical analysis (Figure 7) or by measuring f_N , the nematic fraction present at a given temperature by means of NMR spectroscopy as described in the experimental section. Figure 8 shows the value of f_N as measured by PMR on cooling three different samples from the isotropic phase, with cooling rates of 0.1°/min. It should be pointed out that the $N + I$ biphase is reversible, that is, the value of f_N is the same on heating and cooling and does not change with time at constant temperature.

TABLE V
Enthalpies and Entropies of Transition.

COMPOUND	$\Delta H_{S/N}^*$	$\Delta S_{S/N}^{**}$	$\Delta H_{I/N}^*$	$\Delta S_{I/N}^{**}$
8'DDA8'	67.95	156.2	10.84	22.54
8DDA8	-	-	9.00	18.67
9DDA9-M	-	-	9.37	25.12
ONN-9DDA9	-	-	9.75	26.35
NNO-9AZA9	-	-	2.31	6.58
PAA	-	-	3.52	8.71
(DDA9)#polymer	-	-	17.61	41.63
(AZA9)#polymer	-	-	4.73	11.01
CH ₃ O-B-CO ₂ -C ₆ H ₁₃ (19)	-	-	1.89	4.95
CH ₃ O-B-CO ₂ -C ₇ H ₁₅ (19)	-	-	2.40	6.32

* kJ/Kg
** J/Kg°
maximum value

Alignment in the Nematic Phase

Figure 9 shows the nematic order parameter *S* associated with the mesogen of compounds 9DDA9-M, PAA, and 9AZA9, as a function of an arbitrary reduced temperature (normalized to $T_{NI} = T$ at $f_N = 0.5$). The order parameters developed by ONN-9DDA9 and ONN-9DDA9-d₂₀ are the same as that of 9DDA9-M, but crystallization collapses nematic alignment in the vicinity of 80°C (see below).

The difference between S_{9DDA9} , S_{PAA} , and S_{9AZA9} reflects the difference between their respective entropies of isotropization shown in Table V, once again indicating that the orientational order of the mesogen is dictated by the spacer, as was the case for the corresponding polymers. This is further illustrated in Figure 10, where the

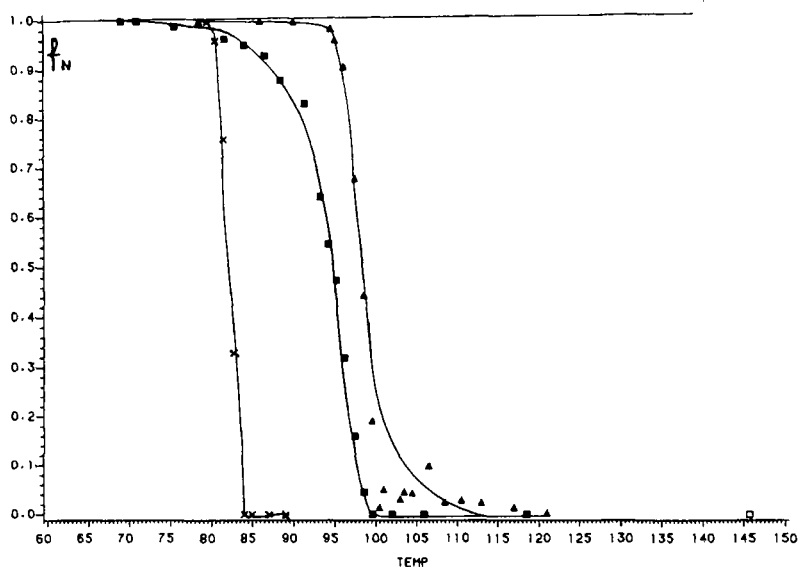


FIGURE 8 Nematic fraction f_N measured by PMR on cooling from the isotropic phase at $0.1^\circ\text{C}/\text{min}$.

x NNO-9AZA9

▲ ONN-9DDA9- d_{20}

■ 9DDA9-M

values of the main dipolar splitting $2\delta_N$ (proportional to S) are plotted as a function of reduced temperature for compounds 9DDA9, 8DDA8 and 8'DDA8'. Figure 10 shows that at constant spacer length ($n = 10$), one obtains roughly the same degree of alignment for all three mesogens.

The values of S and $2\delta_N$ reported in Figure 9 and 10 for 9DDA9 are optimum values achieved under conditions of thermal treatment that allow full development of the nematic phase ($f_N = 1$). This occurs when the sample is first heated some 20 – 25°C beyond the apparent isotropization temperature; that is, the temperature at which the fraction of broad line intensity becomes zero. If, on the other hand, the sample is cooled down from a pretransitional state in which some crystalline nuclei may still be present, nematic alignment is either perturbed or aborted altogether. A similarly crucial influence of sample thermal history on the development of a fully aligned nematic phase was reported previously in the case of mesogen end-capped oligomers of DDA9.⁹ Oriented crystallization of these polymers in strong magnetic fields is also dependent on thermal history.²⁵

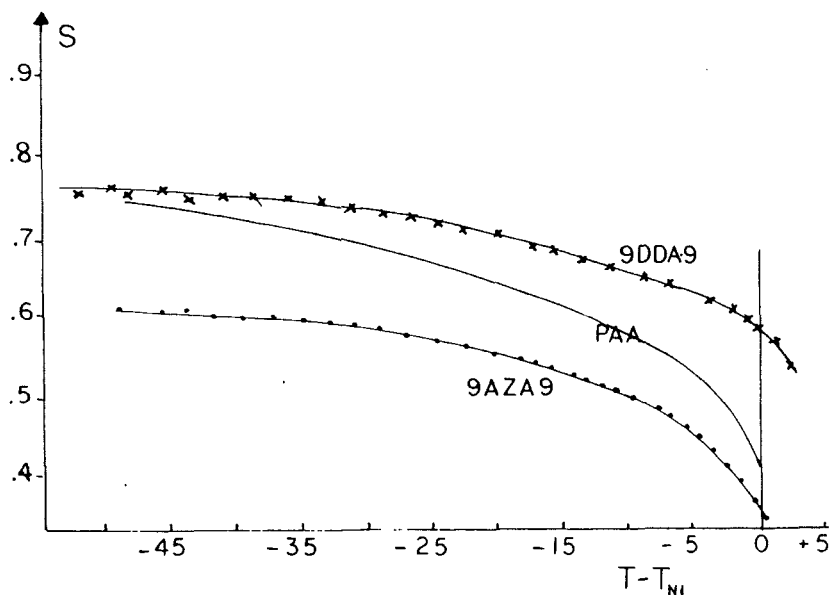


FIGURE 9 Mesogen order parameter of 9DDA9, PAA and 9AZA9, as a function of reduced temperature ($T - T_{NI}$ (°C)). The values of S_{PAA} were obtained from reference 22.

- x 9DDA9-M ($T_{NI} = 95^{\circ}\text{C}$)
- 9AZA9 ($T_{NI} = 82^{\circ}\text{C}$)

Alkyl Chain Flexibility in the Nematic Phase

A deuterium NMR study of polymer DDA9- d_{20} ⁶ and model compound ONN-9DDA9- d_{20} ,²³ both selectively perdeuterated in the spacer moiety, has been published. Figure 11 shows the DMR spectrum of ONN-9DDA9- d_{20} recorded in the homogeneous nematic phase. The two sets of quadrupolar splittings denoted $\Delta\nu_1$ and $\Delta\nu_4$ correspond to the CD_2 groups adjacent to the ester linkage and to all the other CD_2 groups in the spacer, respectively. This implies that the internal methylene groups in the spacer are nearly motionally equivalent. Assuming uniform rotation around the long molecular axis oz_0 , the splitting associated with bond CD_i is

$$\Delta\nu_i(\text{KHz}) = 3/2 \cdot 168 \cdot S < P_2(\cos \beta_i) >$$

where β_i is the angle (CD_i, oz_0), and the brackets represent an average over the internal rotations. As the mesogen order parameter S was independently measured from PMR, the splittings $\Delta\nu_i$ provide a measure of the spacer reorientational mobility, and of its temperature

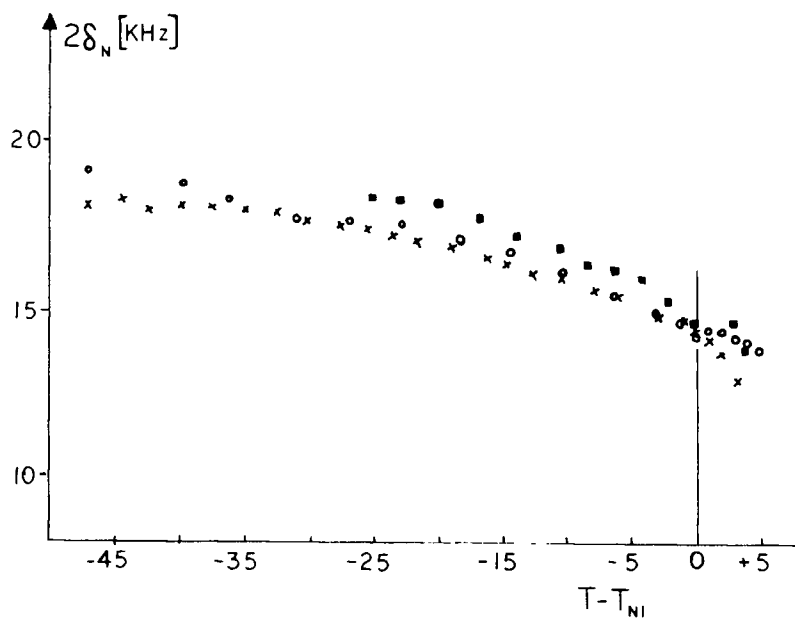


FIGURE 10 Main dipolar splitting $2\delta_N$ as a function of reduced temperature ($T - T_{NI}$ (°C)).

x 9DDA9-M ($T_{NI} = 95^\circ\text{C}$).

■ 8'DDA8' ($T_{NI} = 196^\circ\text{C}$).

○ 8DDA8 ($T_{NI} = 204^\circ\text{C}$).

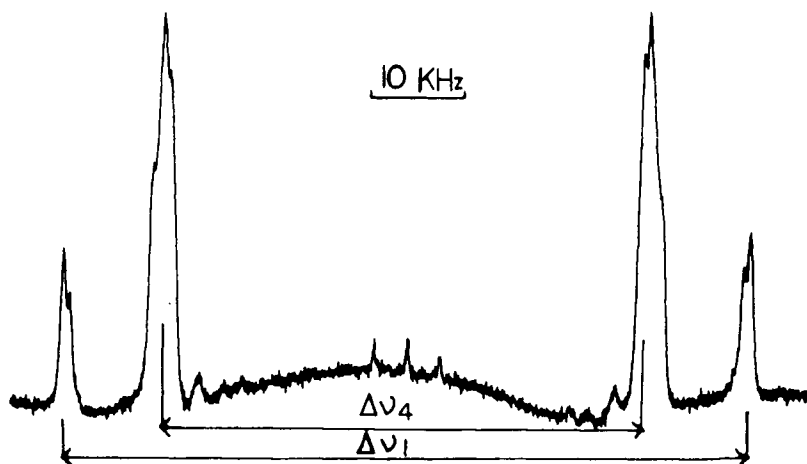


FIGURE 11 Deuterium NMR spectrum of the spacer moiety in ONN-9DDA9- d_{20} at 94°C .

dependence (i.e., a measure of the "internal" order parameter at bond CD_i). For the methylene in α to the ester linkage the internal order parameter was found to be independent of temperature, within experimental error.²³ This simply reflects the well known "trans" geometry of the ester group.²⁴ Rotations around the first C—C bond in the spacer do not change the CD bond orientation relative to oz_0 , forcing $\Delta\nu_1$ to scale directly with S . On the other hand, the internal order parameter of the remaining methylenes decreases with increasing temperature indicating that the spacer disorders faster than the aromatic core, as the N/I transition is approached. Temperature dependence of alkyl chain flexibility was found to be qualitatively similar in the polymer and in the RFR model, and markedly different from that of standard LMM nematics.⁶ Figure 12 shows the temperature

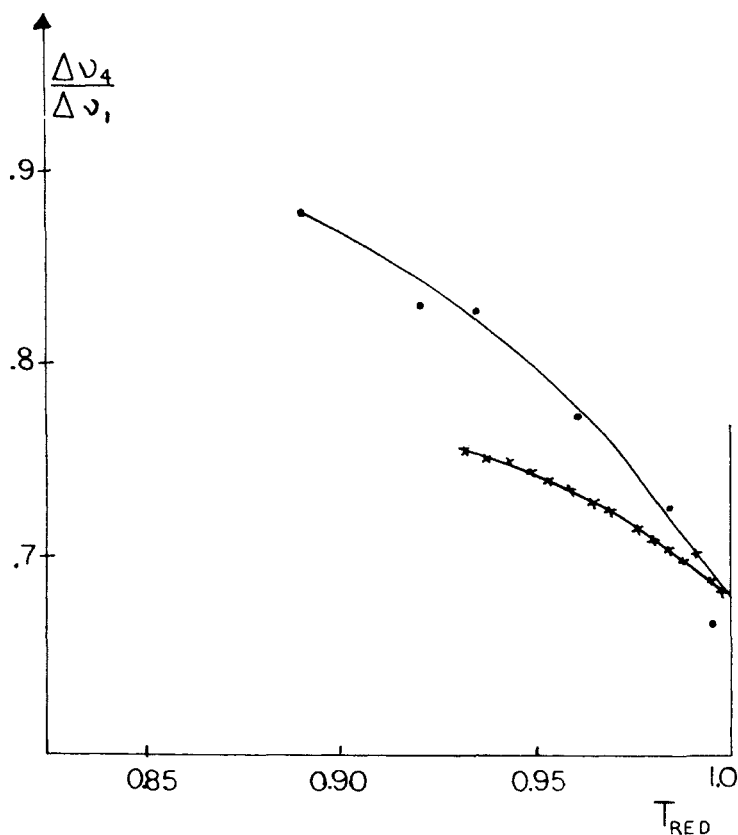


FIGURE 12 Ratio of quadrupolar splittings $\Delta\nu_4/\Delta\nu_1$ as a function of reduced temperature T_{RED} . Upper curve: polymer DDA9-d₂₀ ($\bar{M}_n \sim 3,000$); lower curve: ONN-9DDA9-d₂₀.

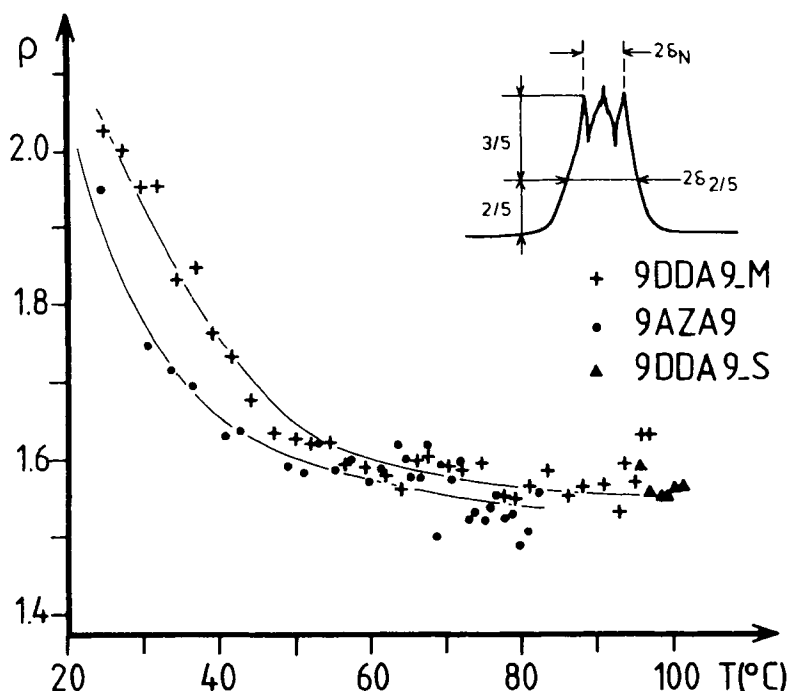


FIGURE 13 Ratio $\rho = \frac{\delta_{2/5}}{\delta_N}$ (defined in the inset) as a function of temperature, on cooling from the isotropic phase.

dependence of the ratio $\Delta\nu_4/\Delta\nu_1$ which provides a visualization of the disordering of the spacer relative to the mesogen. In the DDA9-d₂₀ polymer, the values of $\Delta\nu_1$ and $\Delta\nu_4$ converge markedly as the temperature decreases; in the RFR model, this effect is much less pronounced.

PMR spectra can also be used to visualize this disordering of the spacer, relative to the mesogen, as the N/I transition is approached (Figure 13). In the inset of Figure 13, the main splitting is directly related to the mesogen order parameter S ($2\delta_N/\text{KHz} \sim 24.08 S$), while the distance $2\delta_{2/5}$ at the external shoulders provides a measure of spacer ordering.^{16,23} We can see that the ratio $\rho = \frac{\delta_{2/5}}{\delta_N}$ decreases in

about the same fashion for models 9DDA9 and 9AZA9 as the N/I transition is approached. This indicates that the spacer disorders at about the same relative rate in both compounds, notwithstanding the large difference in mesogen core order due to the odd-even effect.

TABLE VI
Total Enthalpies and Entropies of Fusion.

Compound	ΔH_{total} (KJ/Kg)	ΔS_{total} (J/°Kg)	(ΔS)**	$\Delta S_{\text{IN}} / \Delta S_{\text{total}}$
PAA	113.9	289.6	10.67	0.03
Ac9Ac	113.6	267.9	10.67	--
CH ₃ O-8-OCO-C ₇ H ₁₅	70.75	206.1	5.70	0.03 (19)
9AZA-M#	79.61	257.6	6.23	--
9DDA-M#	84.35	246.2	5.87	--
8DDA8	110.64	240.0	7.44	0.08
9DDA9-M#	96.17	251	7.12	0.10
8'DDA8'	112.64	259.1	7.84	0.09
ONN-9DDA9	107.8	280.0	7.94	0.095
(DDA9)@ polymer	55	135	3.6	0.31
9AZA9 *	--	--	--	--

** (Computed in J/°mole of rigid chain group)

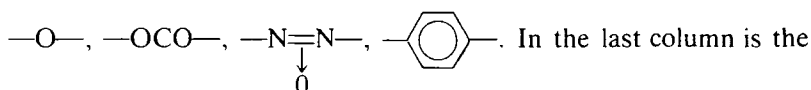
Fully annealed

@ Extrapolated to 100% crystallinity

* Could not be reliably measured, as the nematic phase is supercooled.

Investigation of the Solid Phase

In the first two columns of Table VI are listed the total enthalpy and entropy of fusion for some of the model compounds, computed as the sum of all transitions from K to I. In the third column is the total entropy of fusion expressed in J/°K mole of rigid chain unit,²⁶ where a rigid chain unit is any of the following moieties: CH₃—, —CH₂—,



ratio of entropy of isotropization to total entropy.

Symmetrically substituted mesogens have a total entropy of fusion similar to that expected in a well ordered crystal.²⁶ The RFR siamese twin compounds appear to be somewhat less ordered in their crystalline state, followed by the molecules which in their RF sequencing model the polymer repeat unit. The polymer itself forms the least ordered crystals, as pointed out previously for this and other mesophase polymers.^{26,27,33}

In LMM nematics, the ratio $\Delta S_{NI}/\Delta S_{total}$ is often used to visualize the partitioning of order between the mesophase and the crystal. In LMM nematics this ratio is typically 0.03–0.05, as is the case for PAA and $\text{CH}_3\text{O}-8\text{-OCO}-\text{C}_7\text{H}_{15}$ shown in Table VI. The relatively high values of this ratio for RFR models based on spacer $n = 10$ and its high value for polymer DDA9 reflect both the increased order of the mesophase and the relative disorder of the crystals.

The solid phase of selected compounds was also investigated by wide-line NMR spectroscopy.

Figure 9 shows that in 9DDA9-M the aligned nematic phase can be supercooled to the vicinity of room temperature, in agreement with DSC and microscopy observations. In contrast, pure structural isomers of 9DDA9 crystallize sharply with a concomitant collapse of alignment in the vicinity of 80°C. However, in NNO-9AZA9, the nematic phase is locked in on cooling and a mesophase glass can be formed without subsequent cold crystallization upon reheating. It would seem, then, that the odd-even nature of the spacer might play a role in the kinetics of crystallization of RFR model compounds as it does in corresponding polymers.³³

Figure 14 shows the PMR spectra of ONN-9DDA9- d_{20} obtained on cooling from the N + I biphasic to the crystalline phase (a small fraction of amorphous component appears as a spike on the broad line of the crystal and will be discussed below). Figure 15 shows the transition from an aligned nematic phase of NNO-9AZA9 to a supercooled nematic phase, without loss of alignment. Finally, Figure 16 illustrates the transition from nematic to smectic phase in 8'DDA8'.

The sharp spike of a few hundred Hz in width observed in the PMR spectrum of 9DDA9- d_{20} (Figure 14) represents less than 5% of total intensity. It is also observed in other derivatives of mesogen "9," such as 4,4'-diacetoxy-2,2'-dimethyl azoxybenzene (Ac9Ac). The

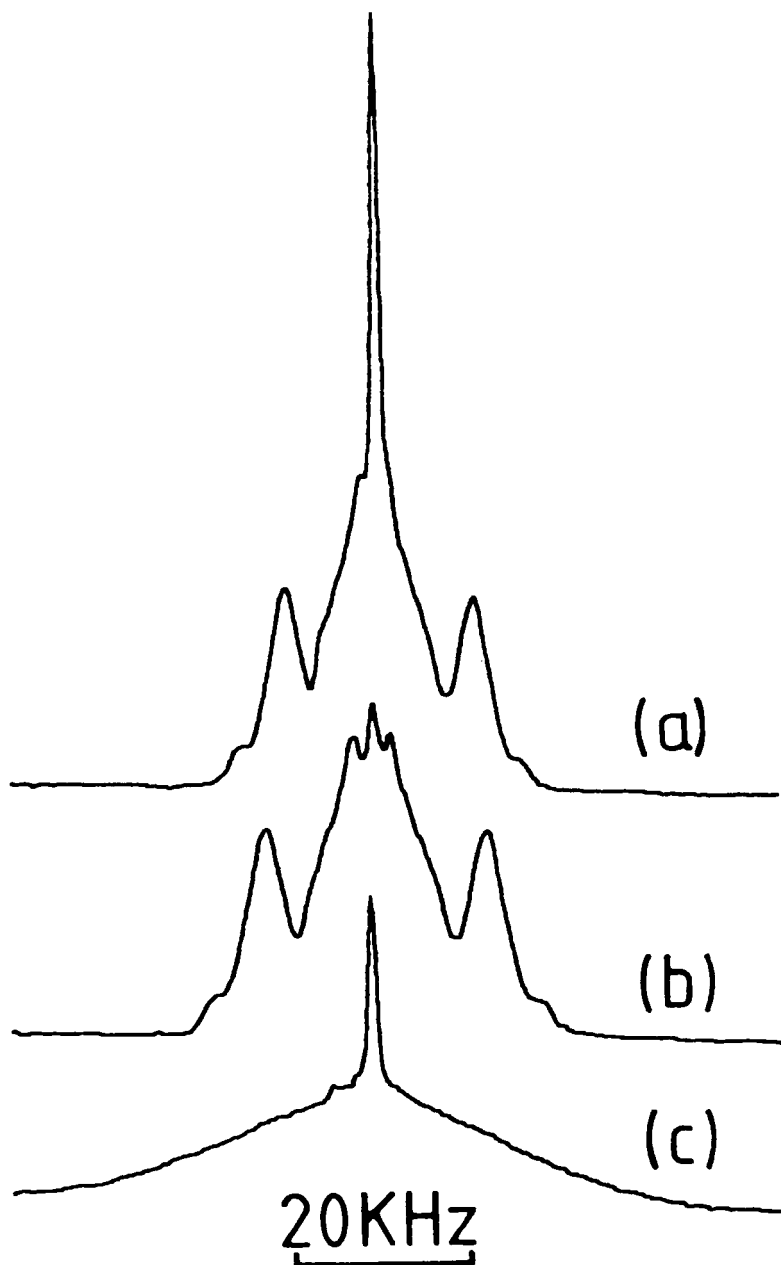


FIGURE 14 PMR spectra of ONN-9DDA9- d_{20} .

a) in the nematic-isotropic biphas (95°C)

b) nematic phase (78.5°C)

c) in the crystal phase (71.5°C)

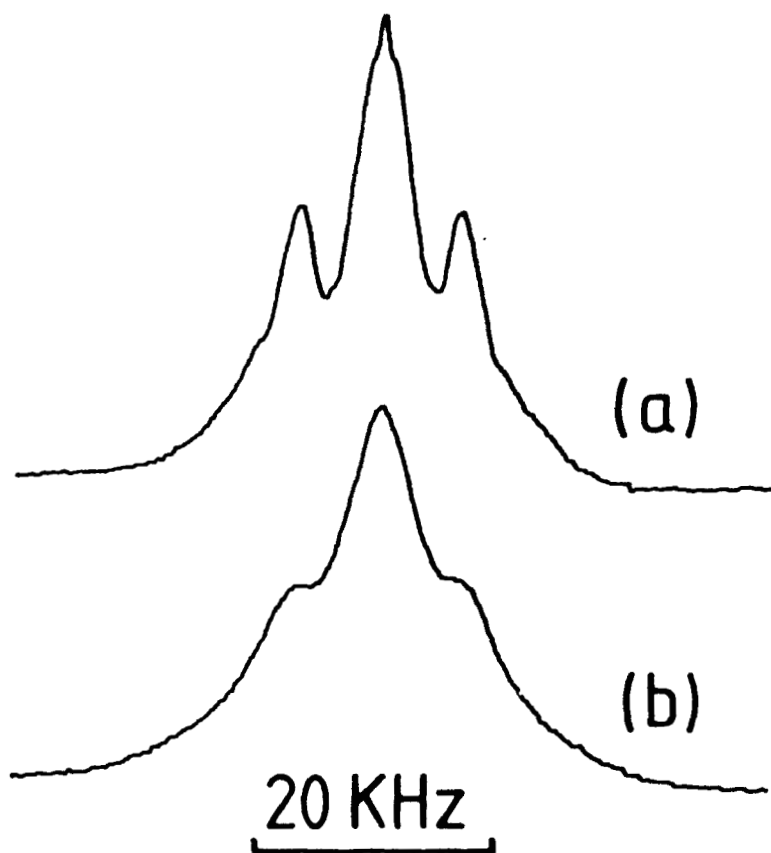


FIGURE 15 PMR spectra of ONN-9AZA9 ($n = 7$).

a) at 41°C.

b) at 25°C.

The nematic phase supercools without loss of alignment.

same sharp component is observed in the deuterium spectrum of 9DDA9- d_{20} .²³ The fraction of the sharp component is the same in PMR and DMR spectra on heating and cooling. As the former “sees” the mesogen and the latter the spacer, this indicates that the entire molecule is partitioned between phases with different mobilities, one of them amorphous.

Compounds 9AZA9 and 9DDA9-M provide the opportunity for investigation of mesophase glasses. Compound 9DDA9-M is interesting to the extent that it tends to form a semicrystalline material and could serve as model for the investigation of the solid polymers.

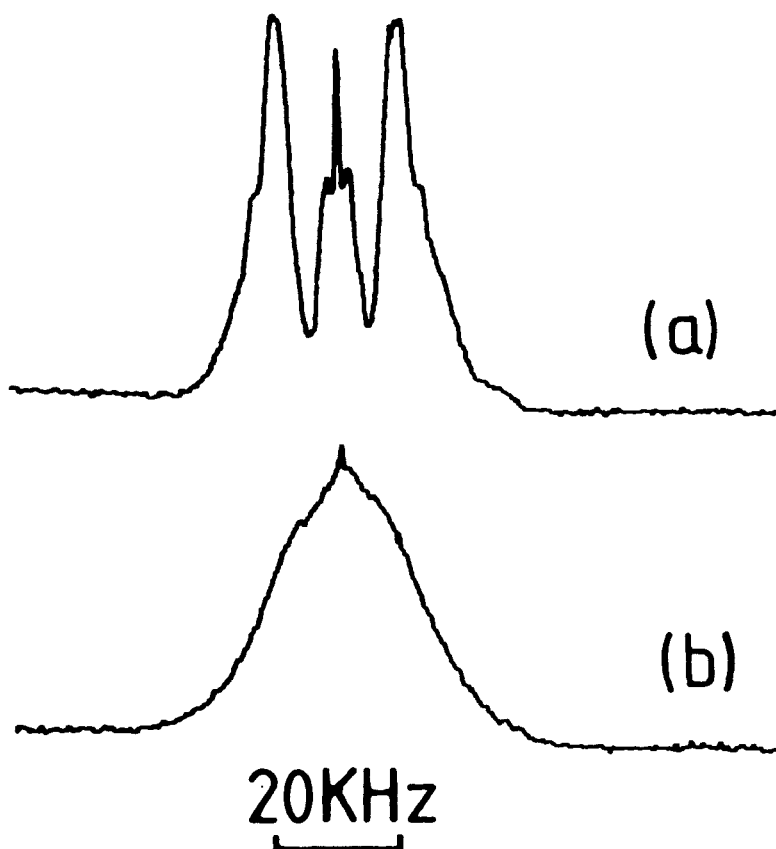


FIGURE 16 PMR spectra of 8'DDA8' (recorded on cooling).

a) 150°C, in the nematic phase

b) 148°C, in the smectic phase

DSC transitions recorded on cooling at 10°/min. are: 1198N153S78K.

The solid phase consists of crystalline and nematic portions. Their relative amounts vary with sample thermal history, as discussed in the section on Multiple Melting. The PMR spectrum of the semi-crystalline material can be decomposed into the contributions of broad and narrow (a few KHz) components, the former due to the crystalline phase and the latter to the unaligned nematic solid.

The line width of the crystalline component remains constant throughout the solid phase at ~20 KHz. The fraction of total intensity contained in the broad component of the NMR spectrum can be measured as explained in the experimental section. A more detailed investigation of the solid nematic phase, above and below the glass transition, will be forthcoming.

DISCUSSION

Siamese twin models with RFR sequencing (mesogen-spacer-mesogen) form the hinge between LMM nematics and nematic PLCs. The orientational order of the mesogen is dominated by the odd-even nature of the spacer, as is the case in the corresponding polymers. Selected RFR models based on spacer DDA ($n = 10$) might have potential applications as low melting, low viscosity "host" molecules with a relatively high degree of nematic order.

The presence of a reversible nematic-isotropic biphasic region observed in RFR models based on spacer DDA ($n = 10$) is difficult to explain at present. Sample purity appears to be adequate (see Experimental Section). Moreover, the biphasic temperature interval at constant concentration of impurity should be inversely proportional to the entropy of isotropization,²⁸ and should consequently be small in these relatively ordered molecules. In addition, if the biphasic region appears as the result of mesophase perturbation by a nonmesomorphic solute impurity, the nematic order parameter should be constant throughout the biphasic region,^{29,30} which is not the case. We tentatively explain this biphasic region by pretransitional effects involving reversible formation of micellar cybotactic clusters in molecules with even membered spacers. The unusual pretransitional behavior of 9DDA9 is reflected in the temperature dependence of the induced magnetic birefringence³¹ and in the temperature dependence of the narrow line of its DMR spectrum.²³ It might also be interesting to point out that a preliminary investigation of 9DDA9 by Fourier transform IR spectroscopy suggests that the mesogens interact more strongly in the nematic phase than in either the solid or the isotropic states, which again would be compatible with cybotactic clustering. The relatively narrow biphasic region of 9AZA9 would be explained by the "ordinary" nematic arrangement of molecules in this odd membered structure. We are currently synthesizing models with the homologous series of spacer lengths to help clarify this point.

Investigation of temperature dependence of alkyl chain flexibility suggests that the spacer disorders more rapidly than the mesogen in both 9DDA9 and 9AZA9. In other words, intramolecular correlation between mesogens appears to stabilize the nematic order of the mesogen in the vicinity of the N/I transition. This effect is more pronounced in the polymer than in the model, but qualitatively the two are similar.

Mixtures of structural isomers in derivatives of mesogen "9" display broad multiple melting at the K/I transition, even in a molecule as long as DDA9DDA9DDA. This multiple melting, and its absence

in corresponding derivatives of mesogen "8," is explained by influence of isomerism on crystalline packing in the 2-2'-dimethyl-azoxybenzene derivatives. A theoretical conformational analysis of the 2,2'-dimethyl-azoxybenzene molecule³² shows that the methyl groups in ortho to the azoxy linkage hinder the possibility of motion around the C—N bonds: conformations in which the azoxy oxygen is too near the methyl groups are forbidden. Interactions between the methyl groups further contribute to the distorted nature of the molecule. As mentioned previously, the model used to fit the experimental PMR spectra of polymer DDA9 also calls for a severely distorted mesogen molecule. Energy barriers between rotational isomers are much greater in mesogen "9" than in mesogen "8,"³² and each structural isomer of "9" is probably frozen in a preferred conformation in the crystalline lattice. In the crystalline state, model compounds that contain a spacer group appear to be conformationally disordered, though not as severely as the polymer itself. Crystallization can be bypassed in some instances and the mesophase supercooled to its glassy state.

In model compounds with RFR sequencing, orientational correlations can propagate intramolecularly via the spacer, as in the corresponding polymers. This connectivity between mesogens accounts for the qualitative resemblance between RFR models and polymers, namely that mesogen order is dictated by the odd-even nature of the spacer. The higher order of PLC, relative to the RFR precursors, suggests that intramolecular correlations can propagate to fairly remote sites.

Acknowledgment

This work was supported in part by the NSF Polymer Program under Grant DMR 8303989 and by NATO Research Grant No. 475.83. The high resolution NMR work was performed at the Worcester NMR Consortium Facility.

References

1. S. Vilasagar and A. Blumstein, *Mol. Cryst. Liq. Cryst. (Letters)*, **56**, 263 (1980).
2. A. Blumstein and O. Thomas, *Macromolecules*, **15**, 1264 (1982).
3. A. Blumstein, S. Vilasagar, S. Ponrathnam, S. B. Clough, G. Maret and R. B. Blumstein, *J. Polym. Sci., Polym. Physics Ed.*, **20**, 877 (1982).
4. A. Blumstein, O. Thomas, J. Asrar, P. Makris, S. B. Clough and R. B. Blumstein, *J. Polym. Sci. (Letters)*, **22**, 13 (1984).
5. A. Blumstein, Proceedings of the 1st International SPSJ Conference, Kyoto, August 1984; *J. Polym. Sci., Japan*, **17**, 277 (1985).

6. E. T. Samulski, M. M. Gauthier, R. B. Blumstein and A. Blumstein, *Macromolecules*, **17**, 479 (1984).
7. R. B. Blumstein and E. M. Stickles, *Mol. Cryst. Liq. Cryst. (Letters)*, **82**, 151 (1982).
8. R. B. Blumstein, E. M. Stickles and A. Blumstein, *Mol. Cryst. Liq. Cryst. (Letters)*, **82**, 205 (1982).
9. R. B. Blumstein, E. M. Stickles, M. M. Gauthier, A. Blumstein and F. Volino, *Macromolecules*, **17**, 2, 177 (1984).
10. The name "siamese twin" is borrowed from A. C. Griffin and T. R. Britt, *J.A.C.S.*, **103**, 4957 (1981).
11. D. Vorländer, *Z. physik. Chem.*, **126**, 449 (1927).
12. N. J. Leonard, J. W. Curry, *J. Org. Chem.*, **17**, 1071 (1952).
13. R. A. Raphael and E. Vogel, *J. Chem. Soc.*, **Pt. 2**, 1958 (1952).
14. S. Vilasagar, *Doctoral Dissertation*, University of Lowell, Lowell, MA, (May 1983).
15. J. Van der Veen, W. H. de Jeu, A. H. Grobбен and J. Broven, *Mol. Cryst. Liq. Cryst.*, **17**, 291 (1972).
16. A. F. Martins, J. B. Ferreira, F. Volino, A. Blumstein and R. B. Blumstein, *Macromolecules*, **16**, 279 (1983).
17. F. Volino, J. M. Allonneau, A. M. Giroud-Godquin, R. B. Blumstein, E. M. Stickles and A. Blumstein, *Mol. Cryst. Liq. Cryst. (Letters)*, **102**, 21 (1984).
18. D. Demus, H. Demus and H. Zashke, *Flüssige Kristalle in Tabellen*, p. 174, VEB, Leipzig (1974).
19. M. T. McCaffery and J. A. Castellano, *Mol. Cryst. Liq. Cryst.*, **18**, 209 (1972).
20. A. Blumstein, K. N. Sivaramakrishnan, R. B. Blumstein and S. B. Clough, *Polymer*, **23**, 47 (1982).
21. J. Asrar, O. Thomas, P. Zhou and A. Blumstein, *Proceedings 28th IUPAC Macromolecular Symposium*, Amherst, MA, p. 797, July 1982.
22. E. G. Hanson and Y. R. Shen, *Mol. Cryst., Liq. Cryst.*, **36**, 193 (1976).
23. F. Volino and R. B. Blumstein, *Mol. Cryst. Liq. Cryst.*, **113**, 1, 147 (1984).
24. P. J. Flory, *Statistical Mechanics of Chain Molecules*, p. 183, Wiley Interscience (1969).
25. G. Maret and A. Blumstein, *Mol. Cryst. Liq. Cryst.*, **88**, 295 (1982).
26. B. Wunderlich, *Macromolecular Physics*, Vol. 3, "Crystal Melting," Academic Press (1980).
27. D. J. Blundell, *Polymer*, **23**, 359 (1982).
28. D. E. Martire in *Molecular Physics of Liquid Crystals*, G. Luckhurst and G. W. Gray, Eds., p. 221, Academic Press (1979).
29. D. H. Chen, G. R. Luckhurst, *Trans. Faraday Soc.*, **65**, 656 (1969).
30. B. Kronberg, D. R. F. Gilson and D. Patterson, *J. Chem. Soc., Faraday II*, **72**, 1673 (1976).
31. G. Maret, *Polymer Preprints*, **24**, 2, 249 (1983).
32. J. Bergès and H. Perrin, *Mol. Cryst. Liq. Cryst.*, **113**, 1, 269 (1984).
33. R. B. Blumstein, O. Thomas, M. M. Gauthier, J. Asrar and A. Blumstein in *Polymeric Liquid Crystals*, A. Blumstein, Ed., Plenum Press, N.Y., p. 239, 1985.